Proceedings of the 2019 5th International Conference on Advances in Electrical Engineering (ICAEE), 26-28 September, Dhaka, Bangladesh

Melanoma Diagnosis from Dermoscopy Images Using Artificial Neural Network

Sharmin Majumder[1], Muhammad Ahsan Ullah[2] and Jitu Prakash Dhar[3]
Department of Electrical and Electronic Engineering[1,2,3]
Chittagong University of Engineering and Technology, Chittagong -4349, Bangladesh[1,2,3]
Email: sharmin@cuet.ac.bd[1], ahsan@cuet.ac.bd[2], jituprakashdhar@gmail.com[3]

Abstract— **Melanoma is the deadliest and unpredictable type of skin cancer. Fortunately, if it is diagnosed and treated at its early stage, the survival rate is very high. To avoid invasive skin biopsy, melanoma diagnosis from dermoscopy images has been introduced for last few decades. But it is very challenging due to low interclass variance between melanoma and non-melanoma images, and high intraclass variance in melanoma images. This paper presents a new approach for diagnosing melanoma skin cancer from dermoscopy images based on fundamental ABCD (Asymmetry, Border, Color, and Diameter) rule which are associated with shape, size and color properties of the images. Two new features related to area and perimeter of the skin lesion are proposed in this paper along with the other existing features which are distinguishing between melanoma and benign images. Dull razor algorithm is applied for black hair removal from the input images and Chan-Vese method is employed for segmentation. The extracted features are applied to an Artificial Neural Network (ANN) model for training and finally detecting melanoma images from the input images. This proposed approach achieves overall accuracy of 98%. This promising result would be able to assist dermatologist for making decision clinically.**

Keywords*— *Melanoma, Skin Cancer, Image Pre-processing, Segmentation, Chan Vese Method, Feature Extraction, Artificial Neural Network.

I. INTRODUCTION

Melanoma skin cancer is the most fatal type of skin cancer although it is not as much of common. The other accounts of skin cancer include the basal and squamous cell skin cancers, although they are not as fatal as melanoma. Despite the fact that this accounts for less than 5 percent of all diagnosed cases of skin cancer, 75% of skin cancer deaths occur due to melanoma [1]. 287,723 new melanoma cases were reported, and 60,712 deaths occurred due to melanoma globally in 2018 [2]. Almost 90% melanomas are associated with excessive UV exposure from the Sun [3]. Melanomas always tend to spread into adjacent lymph nodes, lungs, and brain. But fortunately, if it is identified and treated at its early stage, the survival rate is very high almost 100%. Moreover, biopsy is an invasive, costly and time-consuming technique for cancer detection. Therefore, melanoma diagnosis from dermoscopy images have been a dynamic research area. Automated diagnosis from dermoscopy images includes acquisition of potential images, pre-processing of the input images, segmentation, extraction of distinct and pertinent features and image classification as melanoma or non-melanoma.

The most common rules or methods for melanoma diagnosis are the ABCD rule [4], seven-point checklist method [5], three-point checklist [6], Menzies Method or CASH algorithm [7]. The most widespread screening tool is the ABCD rule [4], [8]. The symptoms of early melanoma are described by the ABCD rule as follows [9]: *Asymmetry*. If the segmented image is split across the major axis, one part doesn't match to the other part of the image in terms of size and shape. *Irregular border*. Melanoma image border generally becomes jawed, uneven, ragged, or blurred. *Color Variegation*. Color variegation in the lesion region is present. Shades of red, black, dark-brown, light-brown, white, or blue-gray may be present. *Diameter*. Malignant lesion usually grows larger, in most cases, it might be larger than 6mm (about 1/4 inch wide). Moreover, changes are also significant over the few weeks or months in malignant melanoma lesion.

The input dermoscopy images may contain hairs or some other artefacts. Dull-Razor algorithm [10], Eshaver algorithm [11], anisotropic diffusion filter [12], median filter etc. are widely used to remove hairs and other noises from the skin images. Otsu thresholding algorithm [13], region merging algorithm [14] [15], active contour method [16] etc. are commonly used algorithms for lesion segmentation from surrounding skin background. Diagnosis accuracy of around 75-84% was reported even when the skilled dermatologists detect melanoma from skin images [17]. In [18], authors mentioned that in case of micro-melanoma diagnosis the ABCD rule became ineffective. Shape, color and texture features were extracted from skin lesion and three classifiers were used to classify melanomas in [19]. Performances of the features were analyzed by both individually and combined in this paper and sensitivity of 98% and specificity of 70% were achieved for texture feature with random forest algorithm for 180 images. Kasmi et al. [20] extracted features based on ABCD rule from 200 dermoscopic images and achieved 91.25% sensitivity and 95.83% specificity. In [21], the authors determined 54 features which include border irregularity, eccentricity, color histogram etc. from 173 images (39 melanoma, 14 nonmelanoma and 120 benign images). This paper gave 97.4% sensitivity and 44.2% specificity. Korjakowska [22] extracted shape, color, and texture features and proposed a feature selection algorithm to classify micro-malignant melanoma with a diameter under 5 mm in their initial stage and achieved 90% sensitivity and 96% specificity using Support Vector Machine (SVM) classifier for 200 dermoscopic images. Some recent papers [23], [24] proposed convolutional neural network (CNN) with large data for melanoma recognition. In 2019, fusion of deep learning and handcrafted method is proposed by Hagerty et al. and 94% overall accuracy was achieved [25].

In this paper, an automated diagnosis system for melanoma recognition from dermoscopy images is developed. Eight features based on shape, size, and color properties are

978-1-7281-4933-2/19/$31.00 ©2019 IEEE

proposed here for melanoma detection and 96.5% overall accuracy is achieved.

II. Proposed Approach

The workflow diagram of the proposed approach is shown in Fig. 1. Here, input images are collected from PH2 dataset.

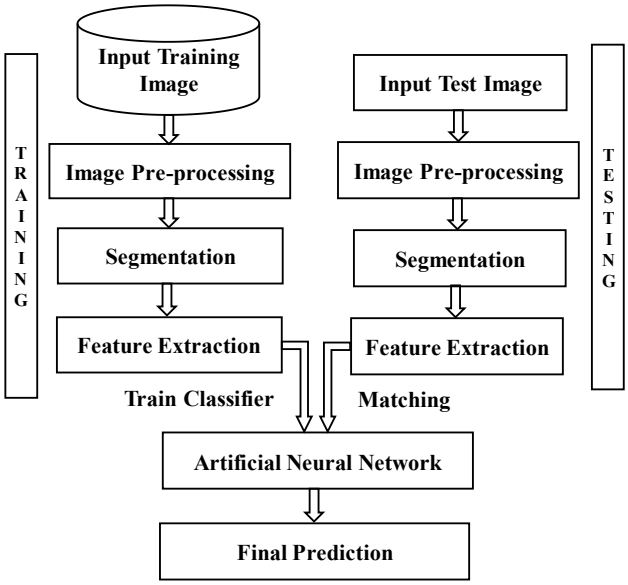

Fig. 1. Pipeline of the proposed approach

These input images are passed through the noise removal block which includes Dull-Razor algorithm for black hair removal and median filter for other noise removal. Afterwards, to separate the lesion from the background skin, active contour segmentation method without edge is applied to these pre-processed images. An ANN model is trained with the features extracted from the 200 images and optimized for further classification. Each step makes a significant impact on the following step. Therefore, all steps must be taken into account with importance. The performance of the proposed system is evaluated by sensitivity, specificity and accuracy.

A. Image Acquisition & Pre-processing

Acquisition of suitable input images to develop a diagnosis system for melanoma is one of the most important tasks. Input training images in this work are collected from PH2 database which was constructed by a combined research association of the University Porto and the Hospital Pedro Hispano, Portugal [26]. The images of this database were obtained in the same conditions through Tuebinger mole analyser system. We have collected 200 melanocytic images which includes 160 benign and 40 melanoma lesion images based on histopathological test. All these images have the resolution of 768×560 pixels. There are 8-bit RGB bitmap format images. The magnification factor is 20x. Two samples for benign and malignant images of PH2 database are shown in Fig. 2. Melanoma images are considered more asymmetrical in shape, irregular, uneven, and jawed shaped borders. Diameter of melanoma image is found greater than 6mm and the image consists of three or more colors.

First step after image acquisition is to remove the hair and artefacts from the input skin images. Human body is covered by hairs as a whole. Moreover, various other noises may be generated during image acquisition by camera. Therefore, pre-processing of these input images is needed to remove the hairs and other noises which will make the following segmentation stage more accurate. To remove black hair, Dull-Razor algorithm [10] is applied and to remove other noises and artefacts, median filter is employed here. Dull-Razor algorithm works based on bi-linear interpolation, grayscale morphological closing operation, and adaptive median filtering. A sample image for hair removal is shown in Fig. 3.

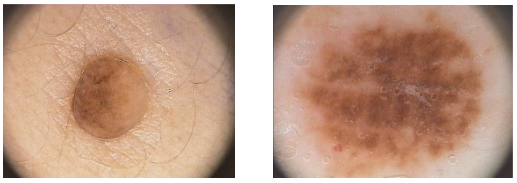

(a) (b)

Fig. 2. Sample input images: (a) common lesion, and (b) melanoma

(a) (b)

Fig. 3. (a): Original image, (b): pre-processed image after hair removal

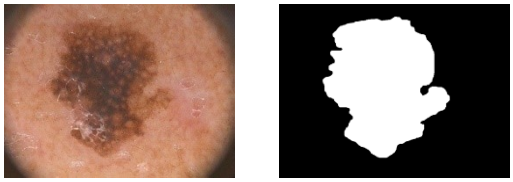

(a) (b)

Fig. 4. (a): A sample pre-processed image, and (b): corresponding segmented image.

B. Image Segmentation

Image segmentation separates the lesion (region of interest) from the surrounding skin background. It is a challenging task due to low grade of interclass variance among lesion and skin background. This step converts graysacle image into binary image containing only skin lesion. In this experiment, active contour method without edge proposed by Chan and Vese [16] is adopted for segmentation. This method works based on energy minimization. An initial contour is selected before around the object. Then the contour moves towards the object by shrinking and expanding itself based on minimization of energy in the image. This contour finally gets stop on the object boundary where energy is minimum, and the required segmented binary image is found. A sample dermoscopy image and its corresponding segmented image are shown in Fig. 4(a) and Fig. 4(b), respectively.

C. Feature extraction

Features are extracted based on ABCD parameters. Here, A, B, and D are associated with shape and size properties and C determines color properties of the lesion images. Two asymmetry scores, three border features, one color feature and two diameter features are considered in this work as distinct and pertinent to distinguish melanoma from non-melanoma. To extract shape features, area, centroid, and orientation angle of the binary image are computed from the moments of the image. Area (A) is specified by the zeroth order raw moment. Perimeter (P) defines the sum of distances between adjacent pair of pixels over the boundary of the object. Centroid presents the centre of mass in the

binary image and Orientation angle is the angle between the major axis of the lesion and *x*-axis of coordinate system.

1) Asymmetry: Asymmetry is one of the most important features for melanoma classification. A melanoma lesion is characterized by asymmetric shape and size. To compute asymmetry, the binary image is first aligned to the image coordinate system by translating its centroid to the origin of coordinate system and then rotating it by the orientation angle. Now the major axis of the lesion is fit onto the *x*-axis of coordinate system. This aligned image is flipped across x-axis. The non-overlapping region between aligned image (T) and flipped image (T_x) is determined by an x-or operation and asymmetry score ($A1$) along *x*-axis is the ratio of the areas of these two images, given by (1). Similarly, the asymmetry score along *y*-axis ($A1$) is also calculated by (2). Fig. 5 presents the steps for determining asymmetry score from a sample image.

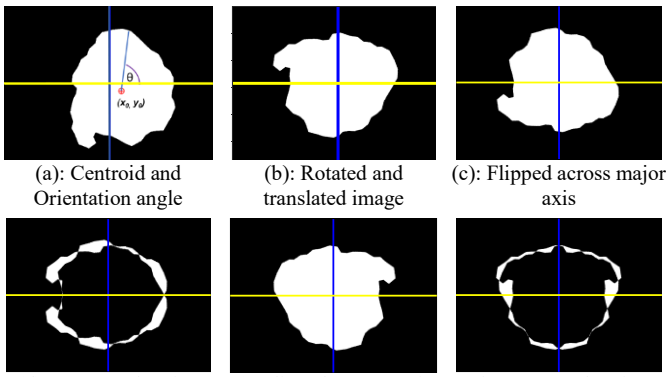

(a): Centroid and Orientation angle | (b): Rotated and translated image | (c): Flipped across major axis

(d): Non-overlapping region between (b) & (c) | (e): Flipped across major axis | (f): Non-overlapping region between (b) & (e)

Fig. 5. Computation of two asymmetry scores

$$T_x = T \oplus T_x, \quad A1 = \frac{\Delta T_x}{\Delta T} \tag{1}$$

$$T_y = T \oplus T_y, \quad A2 = \frac{\Delta T_y}{\Delta T} \tag{2}$$

Here, ΔT_x and ΔT_y are the areas of non-overlapping regions across *x* and *y* axis, respectively.

2) Border Features: Melanoma lesions are considered as irregular, and uneven shaped border. Here, three border features are considered to compute border irregularity. $B1$ specifies circularity index given in (3). This score is 1 for circle and deviates from 1 to 0 for irregular border. Hence, melanoma lesion is found to have low circularity index. Border feature, $B2$ is associated with area and perimeter of the binary lesion, given in (4). Melanoma lesions have larger size as well as complex perimeter and therefore, this score is found greater for melanoma than benign lesions. Border feature $B3$ is calculated from perimeter and average diameter of the lesion. This score is also 1 for circle and greater than 1 for other shapes. Melanoma lesions contain higher $B3$ values in compared with normal lesions.

$$B1 = \frac{4\pi A}{P^2} \tag{3}$$

$$B2 = AP \tag{4}$$

$$B3 = \frac{P}{\pi D} \tag{5}$$

3) Color Variegation: Melanoma images consist of three or more colors whereas benign images contain uniform color [27]. Even, almost 40% malignant images contain five or six colors [22]. Hence, color variegation is one of the most significant parameters of melanoma images. To compute color score (C), six colors are considered here according to PH2 database [26]. These six colors are white, light brown, dark brown, red, blue gray and black, whereas normal lesions contain brown or black colors. Pixel ranges of red, green and blue color channels to constitute these six colors are determined by several combination from considered 200 images. Binary segmented image is overlayed onto RGB color image to obtain segmented color image shown in Fig. 6. This image is scanned thoroughly to determine the number of pixels of the specified six colors. If more than 5% of the total number of pixels in the lesion contains any specific color, then the color is considered to exist, and it adds score 1. Therefore, color score can range from 1 to 6. Fig. 6 is characterized by two images containing color score 1, and 4, respectively.

(a) (b)

Fig. 6. (a): Benign image and (b): Melanoma image containing color score 1 and 4, respectively

4) Diameter: A common sign of early melanoma is growing larger and usually it is greater than 6mm [27]. In this paper, two features are considered to specify diameter. Average diameter ($D1$) is calculated by (6). The calculated diameter from this equation is in pixel.

$$D1 = \sqrt{\frac{4A}{\pi}} \tag{6}$$

$$D2 = a - b \tag{7}$$

Another diameter feature is the difference between principal axes lengths (D2) of the best fitted ellipse of the lesion. Major axis (a) and minor axis (b) of the best fitted ellipse are determined from the second central moments and $D2$ is determine by (7). Rise of $D2$ increases the possibility of malignant melanoma.

D. Artificial Neural Network (ANN) Classifier

After the considered features are extracted from 200 images, next step is to train an ANN classifier. In this paper, feedforward neural network with backpropagation algorithm is employed as classifier. Backpropagation means output dataset of the input images is known before. The calculated output for an input image is compared with the target output and generates an error signal. Weights and biases are continuously updated to minimize this error and the adjustment of weights and biases stop when the minimum error is found. Now this model is ready for further classification. In this work, the ANN structure consists of one

input layer with eight neurons for eight input features, one hidden layer with hundred neurons and one output layer with one neuron as shown in Fig. 7. Output is defined as 0 or 1, where 0 stands for benignity and 1 defines malignancy.

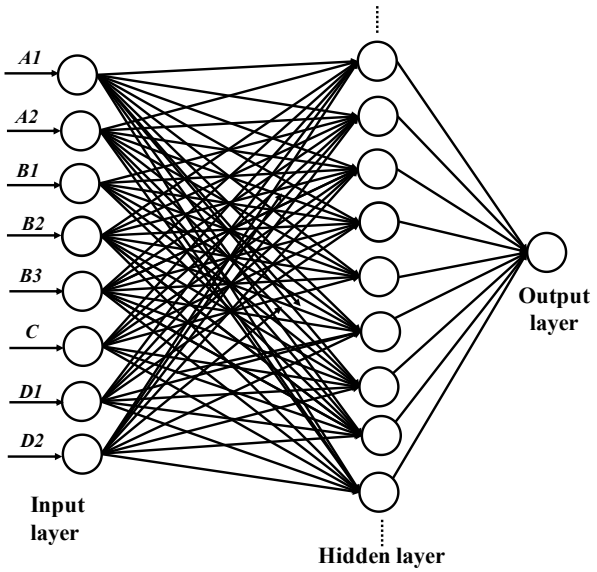

Fig. 7. Structure of Artificial Neural Network used in this work

III. RESULTS AND DISCUSSION

The proposed system has been implemented with MATLAB 2016a. TABLE II presents extracted feature values as well as diagnostic results of five sample benign images and five melanoma images from the input training dataset. The performance of the diagnostic system is analysed by three evaluation parameters: Accuracy, Sensitivity, and Specificity. These three parameters are calculated by 8, 9, and 10.

$$Sensitivity = \frac{tp}{tp + fn} \tag{8}$$

$$Specificity = \frac{tn}{tn + fp} \tag{9}$$

$$Accuracy = \frac{tp + tn}{tp + fn + tn + fp} \tag{10}$$

TABLE I. FEATURE VALUES OF FIVE SAMPLE BENIGN AND FIVE SAMPLE MELANOMA IMAGES

Types of Image	Image no. from [26]	Asymmetry		Border			Color	Diameter	
		A1	*A2*	*B1*	*B2* ($\times 10^8$)	*B3*	(*C*)	*D1*	*D2*
Benign	IMD125	0.09	0.09	0.75	0.8	1.12	2	420	186
	IMD146	0.06	0.14	0.76	0.6	1.11	3	390	147
	IMD147	0.12	0.09	0.82	3.6	1.10	1	667	128
	IMD150	0.08	0.07	0.92	2.7	1.04	2	605	97
	IMD175	0.09	0.11	0.9	1.2	1.05	2	463	89
Meloanoma	IMD417	0.25	0.26	0.9	9.9	1.04	4	946	204
	IMD418	0.28	0.36	0.45	6.5	1.47	3	756	141
	IMD420	0.26	0.27	0.59	8.2	1.26	4	851	204
	IMD426	0.16	0.22	0.76	5.2	1.14	2	730	79
	IMD435	0.15	0.15	0.78	7.9	1.11	4	860	178

Here, *tp, fn, tn, fp* specify true positive, false negative, true negative, and false positive, respectively. Sensitivity defines the percentage of correctly classified melanoma images among all melanoma images whereas specificity specifies the percentage of correctly classified benign images from all benign images. Accuracy means the percentage of correctly classified images. Sensitivity, specificity, and accuracy of the proposed diagnostic system are given in TABLE II. This system gives 98% accuracy with 95% sensitivity and 98.75% specificity.

TABLE II. PERFORMANCE OF THE PROPOSED APPROACH

Classifier outputs	Actual images		Sensitivity	Specificity	Accuracy
	Benign	Malignant			
Benign (160)	*tn*=158	*fn* =2	95%	98.75%	98%
Malignant (40)	*fp* =2	*tp* =38			

System accuracy is also evaluated by *F*-score or *F1*-score. *F*-score is calculated by equation (11) and achieved 95% in this experiment. This evaluation also shows a satisfactory level of results.

$$F\text{-}score = \frac{2tp}{2tp + fp + fn} \tag{11}$$

To test the system developed, diagnosis of two images has been performed that do not belong to the original database. Fig. 8 and Fig. 9 show the test results performed with two images (one benign & one melanoma, respectively) collected from the Internet. The results of the two test images are positive.

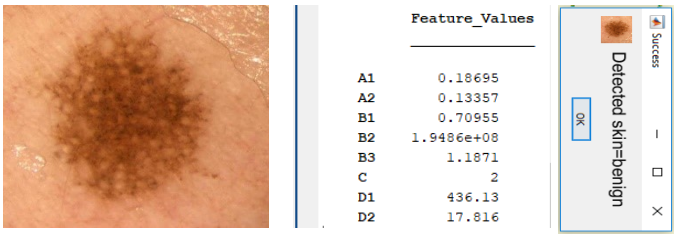

Fig. 8. Test result of a benign image collected from the internet

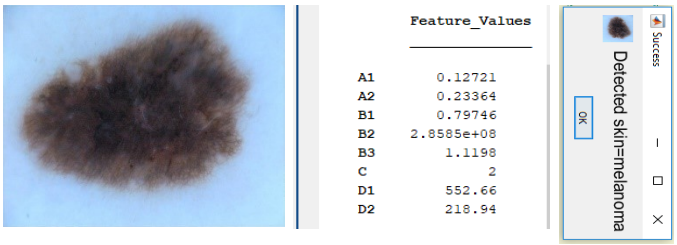

Fig. 9. Test result of a melanoma image collected from the internet

The developed system is also compared with some other published works in terms of classification accuracy although it is difficult to compare with other works because the considered datasets are different. However, TABLE III shows a comparative study of our system with some other relevant works. It is evident from the table that the proposed approach gives a promising result in comparison with the other works.

TABLE III. COMPARATIVE STUDY WITH RELEVANT LITERATURE

Method	Year	Accuracy
[22]	2016	93.24%
[28]	2017	93.6%
[25]	2019	94
Proposed Method	2019	98%

IV. CONCLUSIONS

Melanoma patients have been rising exponentially for the last few years. This paper develops a diagnosis system for melanoma skin cancer which includes eight pertinent features for distinction of melanoma. These features are easy ond fast to calculate which are associated with shape, size and color properties of the input images. This proposed approach gives a satisfactory level of sensitivity and specificity as well as accuracy. Hence, this system could be employed in medical aspect for melanoma diagnosis. However, the limitation of this work is the small size of the database. In future, large dataset will be considered and therefore, deep learning will be taken into account to improve learning and training accuracy.

REFERENCES

[1] C. Lu, M. Mahmood, N. Jha, and M. Mandal, "Automated segmentation of the melanocytes in skin histopathological images," *IEEE J. Biomed. Heal. Informatics*, vol. 17, no. 2, pp. 284–296, 2013.

[2] & J. Bray, F., Ferlay, J., Soerjomataram, I., Siegel, R. L., Torre, L. A., "Global cancer statistics 2018: GLOBOCAN estimates of incidence and mortality worldwide for 36 cancers in 185 countries," *CA. Cancer J. Clin.*, vol. 68, no. 6, p. 394, 2018.

[3] Canadian Dermatology Association, "Melanoma." [Online]. Available: https://dermatology.ca/public-patients/skin/melanoma. [Accessed: 11-Jun-2018].

[4] W. Stolz *et al.*, "ABCD rule of dermatoscopy: A new practical method for early recognition of malignant melanoma," *Eur. J. Dermatology*, vol. 4, no. 7, pp. 521–527, 1994.

[5] D. Singh, D. Gautam, and M. Ahmed, "Detection techniques for melanoma diagnosis: A performance evaluation," *Int. Conf. Signal Propag. Comput. Technol. (ICSPCT 2014)*, pp. 567–572, 2014.

[6] I. Zalaudek *et al.*, "Three-point checklist of dermoscopy: An open internet study," *Br. J. Dermatol.*, vol. 154, no. 3, pp. 431–437, 2006.

[7] J. S. Henning *et al.*, "The CASH (color, architecture, symmetry, and homogeneity) algorithm for dermoscopy," *J. Am. Acad. Dermatol.*, vol. 56, no. 1, pp. 45–52, 2007.

[8] N. R. Abbasi *et al.*, "Early diagnosis of cutaneous melanoma: revisiting the ABCD criteria," *J. Am. Med. Assoc.*, vol. 292, no. 22, pp. 2771–6, 2004.

[9] F. R, Rigel DS, Russak J, "The evolution of melanoma diagnosis: 25 years beyond the ABCDs," *CA. Cancer J. Clin.*, vol. 60, no. 5, pp. 301–316, 2010.

[10] T. Lee, V. Ng, R. Gallagher, A. Coldman, and D. McLean, "Dullrazor: A software approach to hair removal from images," *Comput. Biol. Med.*, vol. 27, no. 6, pp. 533–43, 1997.

[11] K. Kiani and A. R. Sharafat, "E-shaver: An improved DullRazor for digitally removing dark and light-colored hairs in dermoscopic images," *Comput. Biol. Med.*, vol. 41, no. 3, pp. 139–45, 2011.

[12] C. A. Z. Barcelos and V. B. Pires, "An automatic based nonlinear diffusion equations scheme for skin lesion segmentation," *Appl. Math. Comput.*, vol. 215, no. 1, pp. 251–261, 2009.

[13] N. Otsu, "A Threshold Selection Method from Gray-Level Histograms," *IEEE Trans. Syst. Man. Cybern.*, vol. 9, no. 1, pp. 62–66, 1979.

[14] M. Silveira *et al.*, "Comparison of segmentation methods for melanoma diagnosis in dermoscopy images," *IEEE J. Sel. Top. Signal Process.*, vol. 3, no. 1, pp. 35–45, 2009.

[15] A. Wong, J. Scharcanski, and P. Fieguth, "Automatic skin lesion segmentation via iterative stochastic region merging," *IEEE Trans. Inf. Technol. Biomed.*, vol. 15, no. 6, pp. 929–936, 2011.

[16] T. F. Chan and L. A. Vese, "Active contours without edges," *IEEE Trans. Image Process.*, vol. 10, no. 02, pp. 266–277, 2001.

[17] G. Argenziano *et al.*, "Dermoscopy of pigmented skin lesions: Results of a consensus meeting via the internet," *J. Am. Acad. Dermatol.*, vol. 48, no. 5, pp. 679–693, 2003.

[18] C. Marín, G. H. Alférez, J. Córdova, and V. González, "Detection of melanoma through image recognition and artificial neural networks," in *IFMBE Proceedings*, 2015, vol. 51, pp. 832–835.

[19] M. Rastgoo, R. Garcia, O. Morel, and F. Marzani, "Automatic differentiation of melanoma from dysplastic nevi," *Comput. Med. Imaging Graph.*, vol. 43, no. 44–52, 2015.

[20] K. Mokrani and R. Kasmi, "Classification of malignant melanoma and benign skin lesions: implementation of automatic ABCD rule," *IET Image Process.*, vol. 10, no. 6, pp. 448–455, 2016.

[21] L. K. Ferris *et al.*, "Computer-aided classification of melanocytic lesions using dermoscopic images," *J. Am. Acad. Dermatol.*, vol. 73, no. 5, pp. 769–776, 2015.

[22] J. Jaworek-korjakowska, "Computer-Aided Diagnosis of Micro-Malignant Melanoma Lesions Applying Support Vector Machines," *J. Biomed. Biotechnol.*, vol. 6, pp. 1–8, 2016.

[23] L. Yu, H. Chen, Q. Dou, J. Qin, and P. Heng, "Automated Melanoma Recognition in Dermoscopy Images via Very Deep Residual Networks," *IEEE Trans. Med. Imaging*, vol. 36, no. 4, pp. 994–1004, 2017.

[24] J. Premaladha and K. S. Ravichandran, "Novel Approaches for Diagnosing Melanoma Skin Lesions Through Supervised and Deep Learning Algorithms," *J. Med. Syst.*, vol. 40, no. 4, p. 96, 2016.

[25] J. Hagerty *et al.*, "Deep Learning and Handcrafted Method Fusion: Higher Diagnostic Accuracy for Melanoma Dermoscopy Images," *IEEE J. Biomed. Heal. Informatics*, 2019.

[26] T. Mendonca, P. M. Ferreira, J. S. Marques, A. R. S. Marcal, and J. Rozeira, "PH2- A dermoscopic image database for research and benchmarking," *Proc. Annu. Int. Conf. IEEE Eng. Med. Biol. Soc. EMBS*, pp. 5437–5440, 2013.

[27] American Cancer Society, "Melanoma Skin Cancer." [Online]. Available: https://www.cancer.org/cancer/melanoma-skin-cancer. [Accessed: 16-Feb-2019].

[28] F. Dalila, A. Zohra, K. Reda, and C. Hocine, "Segmentation and classification of melanoma and benign skin lesions," *Opt. - Int. J. Light Electron Opt.*, vol. 140, pp. 749–761, 2017.